

## Computer simulation of viscous fingering in a lifting Hele-Shaw cell with grooved plates

SUJATA TARAFDAR<sup>1,\*</sup>, SOMA NAG<sup>1</sup>, TAPATI DUTTA<sup>2</sup>  
and SUPARNA SINHA<sup>1</sup>

<sup>1</sup>Physics Department, Condensed Matter Physics Research Centre, Jadavpur University, Kolkata 700 016, India

<sup>2</sup>Physics Department, St. Xavier's College, Kolkata 700 016, India

\*Corresponding author. E-mail: sujata@phys.jdvu.ac.in

MS received 22 January 2009; accepted 23 May 2009

**Abstract.** We simulate viscous fingering generated by separating two plates with a constant force, in a lifting Hele-Shaw cell. Variation in the patterns for different fluid viscosity and lifting force is studied. Viscous fingering is strongly affected by anisotropy. We report a computer simulation study of fingering patterns, where circular or square grooves are etched on to the lower plate. Results are compared with experiments.

**Keywords.** Viscous fingering; Hele-Shaw cell; simulation.

**PACS Nos** 47.15.gp; 47.20.Gv; 07.05.Tp

### 1. Introduction

Viscous fingering in the lifting Hele-Shaw cell (LHSC) is now a widely studied problem [1–4], because of its academic interest and also due to its application in practical problems such as adhesion [5,6].

The Hele-Shaw cell [7] is a simple apparatus for studying viscous fingering (VF), the instability developed at the interface of fluids of different viscosities [8,9]. The normal HS cell consists of two glass plates separated by a small gap, containing the more viscous fluid. There is a hole in the upper plate, through which the less viscous fluid is forced in.

The LHSC is a modified version of the normal HS cell, where the less viscous fluid enters from the sides, as the plates are drawn apart. The more viscous fluid, sandwiched between the two plates, forms fingering patterns at the interface, under proper conditions [1,4,5]. Different interesting modifications of the HS cell are reviewed in [10].

The effect of anisotropy introduced through patterns on the lower plate of the normal HS cell is well-known [11–13]. Patterns on the lower plate also have a

significant effect in LHSC [14]. The time of plate separation and pattern formation with circular grooves was reported in [14].

Here we present more patterns with an LHSC having square grooves. We try to simulate pattern formation with the grooved plates and compare with the experiments. It is seen that the simulation is able to reproduce qualitative features of the VF formed with square and circular grooves. In the numerical model, the effect of the grooves is considered only by imposing an equalization of the pressure along it. The rationale behind this is the observation in experiments, that once a finger reaches a groove, air immediately spreads all over the groove, indicating equal pressure around the groove.

Even this simplified approach demonstrates the difference between the pressure distribution between plane and grooved plates. The differences in groove patterns also have a significant effect on fingering.

## **2. The LHSC experiment**

The lifting Hele-Shaw cell consists of two plates of toughened float glass. The plates are 10 cm in diameter and 0.5 cm in thickness.

Initially a small volume of fluid measured accurately with the help of an accu-pipette is placed at the centre of the stationary lower plate. The upper plate which is movable is pressed on the lower plate containing the blob of fluid. This creates a situation where a fluid having higher viscosity is surrounded by one with lower viscosity (air in this case) and the combination is sandwiched between two parallel plates. Then the upper plate is slowly lifted, with a constant force keeping it parallel to the lower plate. An air compressor operating a pneumatic cylinder-piston controls the lifting force. The dynamic profile of the moving fluid-air interface is recorded by a CCD camera, placed below the lower glass plate.

In this study, we introduce anisotropy in the set-up, with etched patterns on the lower glass plate. Difference in patterns between (i) a plane glass plate, (ii) a plate with a circular groove and (iii) a plate with a square groove are experimentally recorded. We try to simulate the presence of a groove with a particular symmetry, by introducing a simple modification in the theory as described next. Figure 1 shows patterns generated with this set-up for (A) circular grooved plate, (B) square grooved plate, (C) plane plate with a Newtonian fluid – the olive oil and (D) plane plate with a non-Newtonian paste – oil paint.

## **3. Theory**

In the normal Hele-Shaw cell, usually the invading fluid is air which is assumed to be non-viscous. The pressure distribution in the displaced fluid is obtained as a solution of Laplace's equation [15]. This results from a two-dimensional flow with a constant separation  $b$ , between the plates.

$$\nabla^2 P = 0. \tag{1}$$

Computer simulation of viscous fingering

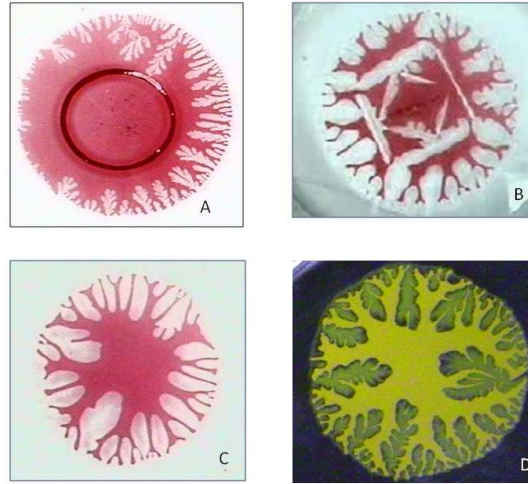


**Figure 1.** Experimentally obtained fingers for (A) circular grooved plate, (B) square grooved plate, (C) plane plate with a Newtonian fluid and (D) plane plate with a non-Newtonian fluid.

However, in the LHSC, the plate separation  $b(t)$  becomes a function of time. The problem can still be considered as a quasi-two-dimensional problem, with  $P$  now a solution of Poisson's equation [2,3].

We follow essentially the approach of Thamida *et al* [2]. The  $z$ -axis is taken normal to the plates and the fluid lies in the  $x$ - $y$  plane. The boundary conditions are: (1) the pressure at the interface of the displaced fluid and invading fluid – air. This is the atmospheric pressure  $P_0$ , (2) the pressure at the centre, which is a parameter  $-p_0$ . The pressure integrated over the whole area  $a$  of the displaced fluid is the constant lifting force  $-F$ .

$$\int P \, dx \, dy = -F. \quad (2)$$

Since the volume of the fluid, assumed incompressible, is a constant  $V_0$

$$V_0 = a(t)b(t). \quad (3)$$

Starting with the continuity equation for the incompressible fluid

$$\nabla \cdot \mathbf{u} = 0, \quad (4)$$

where  $\mathbf{u}$  is the velocity of the fluid. Invoking the thin film lubrication approximation, one has

$$\frac{\partial u_z}{\partial z} = \frac{1}{b} \frac{db}{dt}. \quad (5)$$

Darcy's law relates the lateral fluid velocity to the local pressure gradient as

$$u_x = -\frac{b^2}{12\mu} \frac{\partial P}{\partial x} \quad (6)$$

and a similar relation for  $u_y$ . Here  $\mu$  is the viscosity of the higher viscosity fluid. Finally the Poisson equation to be solved is

$$\nabla^2 P = -\frac{12\mu}{a_0^2} a \frac{da}{dt}. \quad (7)$$

Here,  $a_0$  is the initial area occupied by the higher viscosity fluid.

The above equations cannot be solved analytically, beyond a very short time interval. We solve the equations numerically, to simulate the growth of fingers, and the details are given in the next section.

The presence of grooves makes the situation considerably complex. At present we consider one groove only, either circular or square. The presence of the groove has an equalizing effect on the contour with the desired shape. Other factors, like the change of fluid depth at the groove, are ignored.

#### 4. Computer simulation algorithm

In conformity with the symmetry of the set-up, we formulate the problem initially in polar coordinates. The plates are considered to be circular with radius  $r$ .  $r$  varies from 1 to 30 and  $\theta$  from 0 to 180. The polar coordinates of the system are then converted to Cartesian coordinates. We have thus a circular arrangement of sites on a square lattice.

A random initial disturbance is allowed, to introduce stochasticity in the fingering process. Each site on the circular boundary has an indentation varying randomly between 0 and 3 units. The indentations may be the beginning of a finger, initiated due to thermal noise, or from surface irregularity.

##### 4.1 Plane lower plate

In the case of a plane lower plate, the algorithm is as follows:

- (1) Fluid sites occupying a circular area  $a_0$  are marked by an index 1 and sites occupied by air are marked by 0.
- (2) The boundary conditions are set as a constant pressure (atmospheric, taken as 0) at the outer periphery of the fluid and a negative value  $-p_0 = p_{00}$  at the centre.  $\mu$ ,  $a_0$  and  $p_{00}$  are parameters determining the initial conditions.
- (3) Laplace equation is solved, to get the initial pressure distribution and the pressure at each site is added to give the total lifting force  $-F$ . Darcy's law (eq. (6)) is used to find the fluid velocity at each site, from the pressure gradient.
- (4) The outer periphery is updated by allowing the fluid to move according to the velocity obtained in the previous step.

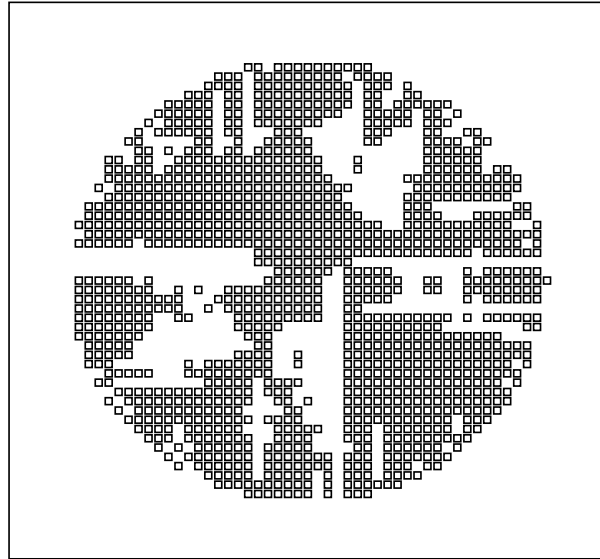


**Figure 2.** A viscous fingering pattern generated by simulation of the lifting process or constant force, with viscosity parameter 0.014.

- (5) Since  $F$  must be maintained constant, the pressure at the centre  $-p_0$  is increased in steps, until the pressure distribution is such that the condition,  $\sum P(x, y) = -F$ , is satisfied for the updated pressure  $P(x, y)$  at each site.
- (6) Now the pressure distribution is updated solving Poisson's eq. (7) taking into account the new area. A suitable time interval  $\delta t$  is chosen as the unit of time. So  $(a_{t+1} - a_t)/\delta t$  is the rate of change of area in eq. (7). Each time the pressure distribution changes, the constant force condition  $\sum P(x, y) = -F_0$  is re-established, by manipulating  $-p_0$ .
- (7) Darcy's law is again invoked to get the fluid velocities, and steps 4 to 6 are repeated as long as necessary to map the evolving fluid boundary and hence the finger growth. Figures 2 and 3 show fingering for two different values of  $\mu$  generated from the above algorithm.

#### 4.2 Grooved lower plates

We have simulated the fingering when there is a single circular or square groove etched on the lower plate. The simulation algorithm is as follows: We assume that the pressure along the groove is equal, i.e. there is an isobar having the shape of the groove in the system. As already discussed, this is borne out by experiment. The pressure on the isobar of course changes with time.

The details of the simulation algorithm for the grooved plate problem will be clear from the flowchart shown in figure 4. The essential modifications of the simulation algorithm are as follows. We initially calculate the pressure distribution from Laplace's equation with boundary conditions as before, forgetting about the

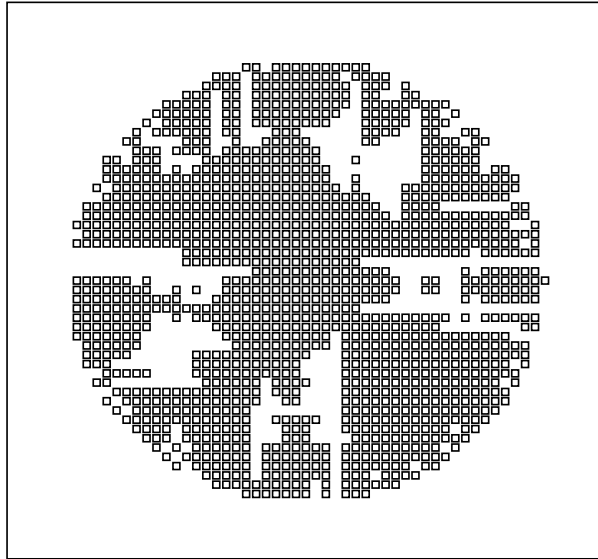


**Figure 3.** A viscous fingering pattern generated by simulation of the lifting process or constant force, with viscosity parameter 0.015.

groove. Then we calculate the average of the pressure over all the groove sites and re-assign that average value to all groove sites.

As before, the condition for constant lifting force is maintained through the condition  $\sum P(x, y) = -F$ , ensured by adjusting  $p_0$ . In the lifting step, pressure is calculated from Poisson's equation, with the appropriate pressure at the centre and groove pressure equalized as before. In the step when the fingers actually advance, according to Darcy's law, we use Laplace equation with the groove (having the equally distributed pressure previously determined) as the inner boundary and the outer fluid-air interface with 0 pressure as the outer boundary. Here Laplace is used instead of Poisson, since the increased height for this step has already been taken into account. These steps are repeated as long as at least one of the fingers touches the groove (refer to figure 4).

Results for circular fluid blobs of radius 24 (in arbitrary units) and a circular groove of radius 8 (in arbitrary units) have been simulated. For a plate with a square groove, exactly the same procedure is followed. Figures 5 and 6 show respectively typical patterns for fingering in a circular grooved plate and a square grooved plate, the groove having a side 16 units long. The simulation is continued until the fingers reach the groove.

It is to be noted that, in each time-step after the initial time-step, the pressure  $P(x, y)$  is calculated first from Poisson's equation, in order to get the average pressure along the groove. Force conservation is ensured, and then the pressure distribution is again calculated from Laplace equation with the groove as the inner boundary. This pressure distribution is used in Darcy's law to get the interface velocity. The actual advancement of the fingers, occurs of course, only once in a time-step.

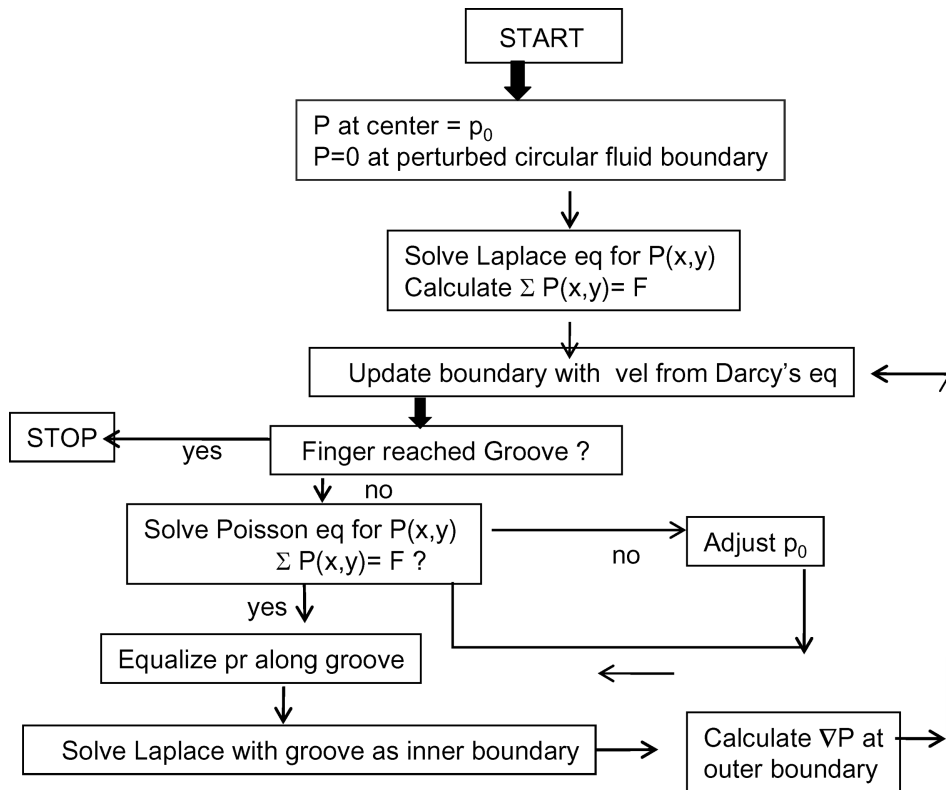


**Figure 4.** Flow chart illustrating the sequence of steps followed for the simulation of the grooved patterns.

## 5. Results

We have studied the development of fingers on a fluid blob of radius 24 units. The results we have presented are for  $\mu = 0.014-0.017$ . The initial central pressure  $p_{00}$ , which determines the lifting force has been varied from 13 to 15. All parameter values are in arbitrary units. For still lower pressure there is no fingering.  $\delta t$  has been taken as 0.7, and this makes the finger advancement length optimum. There is scope for variation of parameter combinations to look at larger sized systems.

We have chosen the parameter values such that about 5–10 time-steps take the fingers to the centre for the plane plate. Since fingers are advanced in discrete steps determined by the velocity, a velocity less than 1 means no advancement in that step.

### 5.1 Plane plate

Changes in the pattern due to variation of  $\mu$  is shown in figures 2 and 3 for  $\mu = 0.014$  and 0.015 respectively, with  $p_{00} = 14.6$ . The plate separation at each time-step can

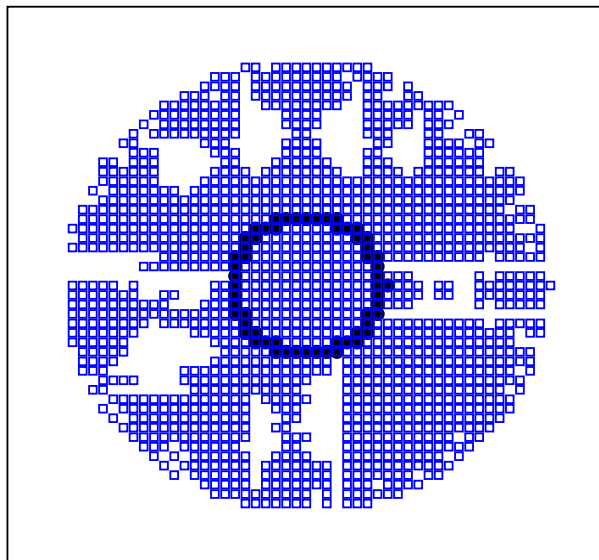


**Figure 5.** Simulated fingering pattern for a circular grooved plate. The pattern is developed in 5 time-steps, after that fingers touch the groove. See text for more details.

be calculated from the inverse of the area covered by the fluid, since the volume of fluid is constant. We find that the separation increases exponentially and some results are shown in figure 7.

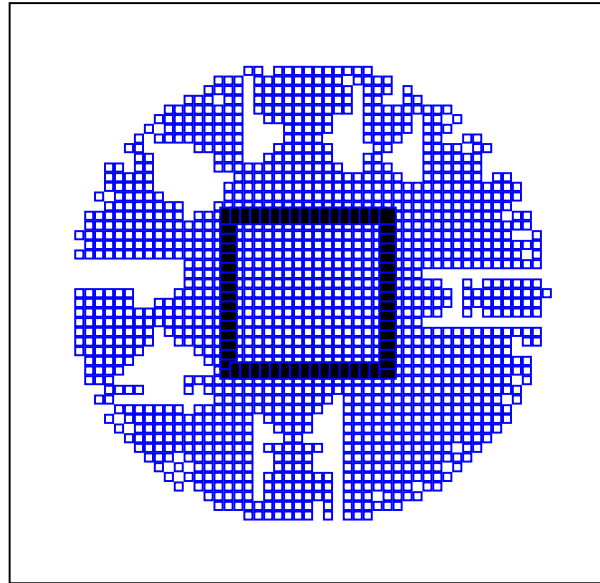
Interestingly, the experimental results also show an exponential increase [16], though this is not predicted from theory [2]. Experimentally obtained plate separation, also calculated from the volume divided by area of contact of the fluid, as a function of time is shown in figure 8. The exponential fit is also shown.

Figure 9 shows the variation of the fluid area of contact, as a function of  $\mu$ . For smaller  $\mu$ , fingers penetrate more and the area of contact decreases strongly.

### 5.2 Grooved plate results

The groove diameter for the circular groove and the side for the square groove are chosen as 16 units. For smaller values, the effect of the groove is much less noticeable, and for larger values, it comes too close to the periphery.

In the present report, we stop the simulation as soon as the groove is reached, but the study can be extended to let secondary fingers proceed from the groove to the centre. Multiple grooves as shown in figure 1D can also be introduced in future. However, for the present simple case, results are already quite interesting. Salient features are discussed in the next section.



**Figure 6.** Simulated fingering pattern for a square grooved plate. The pattern is developed in 5 time-steps, till fingers just touch the groove. See text for more details.

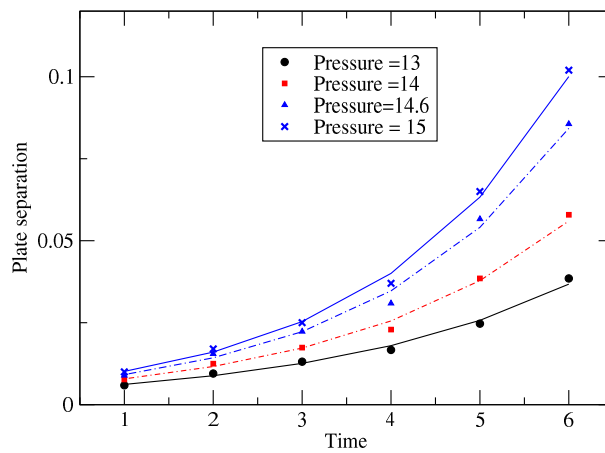


**Figure 7.** Simulated plate separation as a function of time for several lifting pressures are represented by the symbols, the lines are exponential fits. All quantities are in arbitrary units.

## 6. Discussion

At a glance figure 2 shows that the fingers formed look quite realistic, when compared with experimental results shown for the plane plates in figure 1. The initial broadening and later tapering nature of the fingers is reproduced, as is the

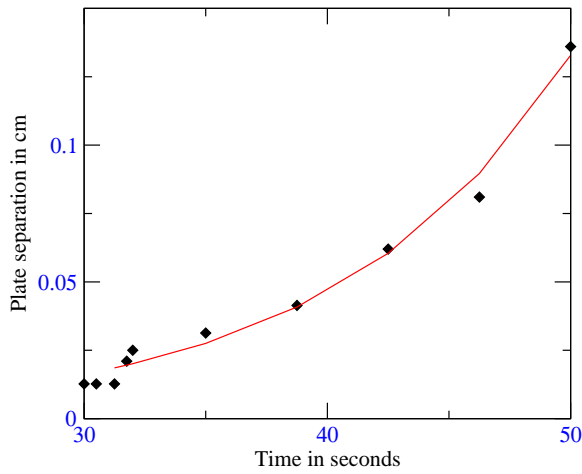


**Figure 8.** Experimental plate separation as a function of time is represented by the symbols, and the line is the exponential fit.

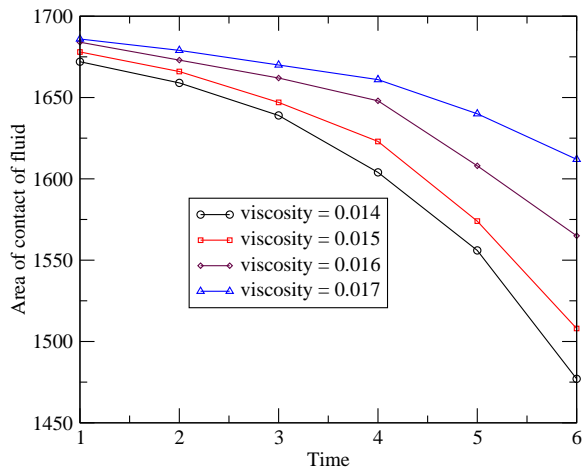


**Figure 9.** Simulated area of contact of fluid, as a function of time for varying viscosity is shown. All quantities are in arbitrary units.

suppression of several fingers due to screening. The imposition of the square geometry makes the finger boundaries somewhat artificially jagged at some places. Smoother contours may be obtained by taking larger systems with a finer mesh of points, thus requiring more computer memory. The simulation pattern looks more like the non-Newtonian fingering in this respect, though of course non-Newtonian nature has not been included in the theory.

On comparison with the simulated grooved patterns, figures 5 and 6, with A and B in figure 1, we see that the essential features introduced by the grooves are reproduced. The circular groove stabilizes pressure gradients and makes more fingers grow longer, compared to the plane plate patterns.

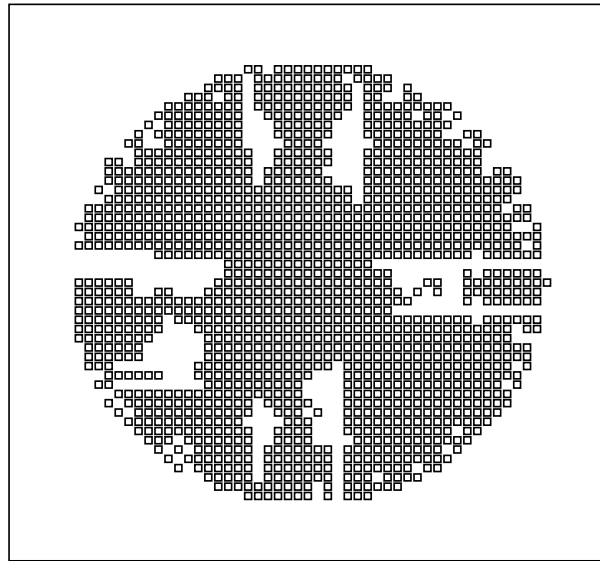


**Figure 10.** Simulated fingering pattern for a plane plate under the same conditions as for figures 5 and 6. The pattern developed in 5 time-steps shows much slower growth of fingers than for the grooved plates.

The difference between the square and circular grooved patterns is also noticeable. In figure 1, experiments show that with the circular groove, all fingers grow more or less equally, while with the square groove, the growth is favoured towards the corners. This is expected, since the pressure gradients are stronger here. Looking at figures 5 and 6, we see that this is exactly the case in the simulation too. The simulated patterns shown have same initial conditions and all other parameters are the same, to facilitate comparison. The time for growth is 5 time-steps. Another striking result is that with grooves, the rate of growth is somewhat enhanced. Figure 10 shows the situation after 5 time-steps for the plane plate, the fingers are much smaller here, compared to figures 5 and 6, also taken after 5 time-steps. This seems to bear out the report of faster growing fingers with grooves, in [14]. However, a comparison between simulation and experiment is rendered difficult by the fact that the extra fluid and larger depth at the grooves cannot be taken into account. The assumption that the same volume of fluid with and without grooves will produce an initial blob with the same radius cannot be true in reality.

To conclude, the complex viscous fingering process with grooved plates can be generated by a simple computer algorithm. It appears that the major effect of the grooves is manifested through a redistribution of pressure, rather than a local change of depth. Another effect is the change in speed of finger growth.

Viscous fingering with anisotropy has been simulated by [13], but that is for the normal HS with a network pattern. Fingering in LHSC with ferrofluids has also been simulated [17]. To our knowledge, this is the first attempt at simulating fingering with etched plates in the LHSC and the results are encouraging.

## Acknowledgement

Authors are grateful to DST for supporting this work, through R/P No. SR/S2/CMP-22/2004. S Sinha thanks DST for a research grant.

## References

- [1] C Gay and L Leibler, *Phys. Today* (Nov.) (1999)
- [2] S K Thamida, P V Takhistov and H C Chang, *Phys. Fluids* **24**, 8 (2001)
- [3] M J Shelley, F-R Tian and K Wlodarski, *Nonlinearity* **10**, 1471 (1997)  
A Lindner, D Derks and M J Shelley, *Phys. Fluids* **17**, 072107 (2005)
- [4] S Roy and S Tarafdar, *Phys. Rev.* **E54**, 6405 (1996)
- [5] S Sinha, T Dutta and S Tarafdar, *Eur. Phys. J.* **E25**, 267 (2008)
- [6] M Tirumkudulu and W B Russel, *Phys. Fluids* **15**, 6 (2003)
- [7] H J S Hele-Shaw, *Nature (London)* **58**, 34 (1898)
- [8] T Vicsek, *Fractal growth processes* (World Scientific, Singapore, 1989)
- [9] M Daoud and H Van Damme, in *Soft matter physics* edited by M Daoud and C E Williams (Springer-Verlag, Berlin, 1999)
- [10] K V McCloud and J V Maher, *Phys. Rep.* **260**, 139 (1995)
- [11] Y Couder, F Argoul, A Arneodo, J Maurer and M Rabaud, *Phys. Rev.* **A42**, 3499 (1990)
- [12] A G Banpurkar, A S Ogale, A V Limaye and S B Ogale, *Phys. Rev.* **E59**, 2188 (1999)
- [13] J-D Chen and D Wilkinson, *Phys. Rev. Lett.* **55**, 1892 (1985)
- [14] S Sinha, S K Kabiraj, T Dutta and S Tarafdar, *Eur. Phys. J.* **B36**, 297 (2003)
- [15] M Ben Amar and D Bonn, *Physica* **D209**, 1 (2005)
- [16] S K Kabiraj and S Tarafdar, *Physica* **A328**, 305 (2003)
- [17] M Oliveira and J A Miranda, *Phys. Rev.* **E73**, 036309 (2006)